Catalysis Letters (2023) 153:3433–3441
https://doi.org/10.1007/s10562-022-04245-3

Facile Fabrication of Hierarchical SAPO-34 in Bifunctional Catalyst for Direct Conversion of Syngas into Light Olefins

Xiaona Wei[1] · Long Yuan[1] · Wenshuang Li[1] · Shitong Chen[1] · Zhiqiang Liu[1] · Shimin Cheng[1] · Li Li[1] · Chuang Wang[1]

Received: 10 October 2022 / Accepted: 9 December 2022 / Published online: 17 December 2022

Abstract

Direct synthesis of light olefins from syngas (STO) using bifunctional catalyst composed of oxide and zeolite has attracted extensive attention in both academia and industry. In this study, we present a facile post-treatment approach to obtain hierarchical SAPO-34 by treating the crystallized product in mother liquor at low temperature. The physical and chemical properties of the resulting molecular sieves were characterized by XRD, SEM, TEM, N_2 adsorption–desorption, XRF and NH_3-TPD. The obtained hierarchical SAPO-34 were mixed with ZnCrAlOx oxide to prepare the bifunctional catalyst, and the catalytic performance for direct conversion of syngas to light olefins was examined. Compared with the bifunctional catalyst obtained from the SAPO-34 molecular sieves without post-treatment, the bifunctional catalyst with hierarchical SAPO-34 obtained by mother liquor post-treatment showed enhanced performance with higher selectivity of light olefins. Importantly, the bifunctional catalyst with hierarchical SAPO-34 has a good catalytic stability with no obvious deactivation over 100 h of testing. The enhanced catalytic performance of the bifunctional catalyst with hierarchical SAPO-34 could be attributed to the hierarchical structure of SAPO-34 that can increase the rate of mass transfer to avoid further hydrogenation and conversion of olefin products on the catalyst, thus could improve the selectivity of C_2–C_4 olefins.

Graphical Abstract

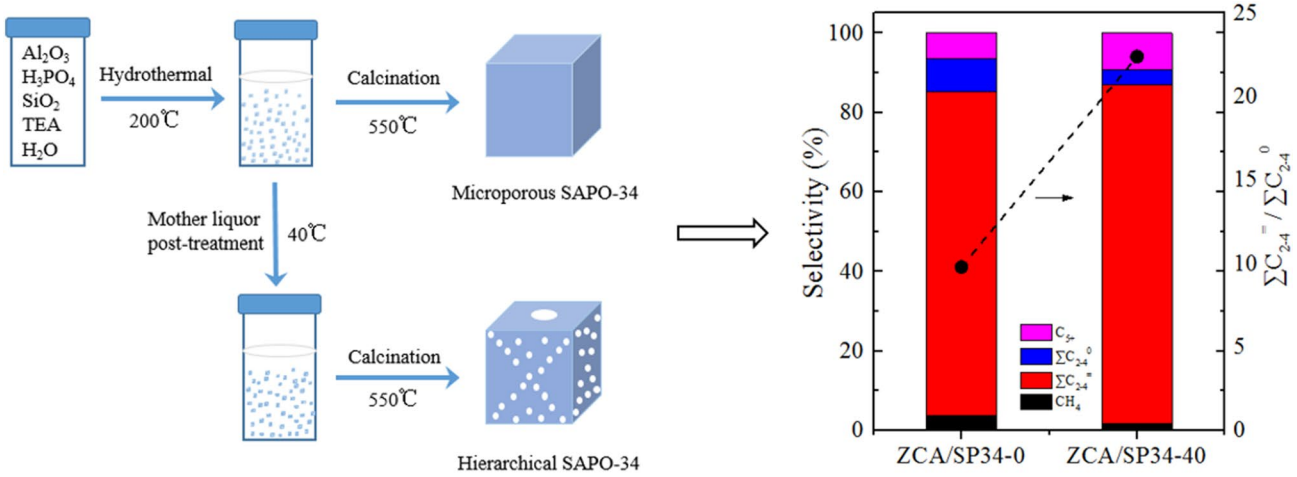

Keywords Hierarchical SAPO-34 · Mother liquor · Bifunctional catalyst · Syngas · Light olefins

Extended author information available on the last page of the article

1 Introduction

Light olefins (C_2–$C_4^=$) are one of the most important basic chemicals, which are widely used in the fabrication of plastics, drugs, solvents, coatings and other commodities [1, 2]. At present, light olefins are mainly produced via the thermal cracking of naphtha and fluid catalytic cracking (FCC) [3, 4]. With the increasing demand for basic chemicals and the reduction of oil reserves, alternative routes has been developed to meet the growing demand for hydrocarbon fuels and chemicals, and to reduce the heavy dependence on oil resources [5]. In this context, the conversion of carbon-based resources such as coal, natural gas, biomass and even industrial waste into fuels and chemicals has aroused new research interests. In practical applications, these carbonaceous feed-stocks are usually converted into syngas (a mixture of H_2 and CO) and then into final hydrocarbon products [5–9]. As an important part of C1 chemistry, the selective conversion of syngas to light olefins is attractive but also challenging in both academic and industrial fields. Currently, indirect and direct methods are used to prepare light olefins from syngas. The indirect method has been successfully commercialized, i.e., first convert syngas to methanol, and then to olefins through methanol to olefin technology (known as MTO) [10]. However, the route of direct conversion of syngas to light olefins should be more cost-effective and energy-efficient because it reduces operating units and, therefore, this route also has attracted extensive attention. In this method, modified Fischer Tropsch synthesis (FTS) catalysts are used, which have been extensively studied for decades. Although remarkable progress has been made in the synthesis of FTS catalysts and in the fundamental understanding of the reaction mechanism of directly converting syngas into light olefins through FTS, it is still difficult to make a major breakthrough in the selectivity of light olefins in the reaction product.

In 2016, Jiao et al. reported a concept of oxide-zeolite (OX-ZEO), using a bifunctional catalyst with partially reduced ZnCrOx and mesoporous SAPO-34 molecular sieves. The light olefins selectivity up to 80% can be achieved over the bifunctional catalyst, which was far beyond the Anderson-Schulz-Flory (ASF) limit [11]. Then, a series of other oxide-zeolite (OX-ZEO) bifunctional catalysts yielding a high selectivity of light olefins were reported, including ZnO–ZrO_2&SAPO-34, MnOx&SAPO-34, ZnO&SAPO-34, Zr–In_2O_3&SAPO-34, Cr–Zn&SAPO-34, ZnAlOx&SAPO-34, $Zn_xCe_{2-y}Zr_yO_4$&SAPO-34, MnGa&SAPO-34, Zn–Cr@SAPO-34, Zn–ZrO_2&SSZ-13, ZnCrOx&MOR, ZnCrOx&low Si content AlPO-18 and so on [8, 12–24]. SAPO-34 is the most widely used catalyst for MTO reaction and is also a component of bifunctional catalyst for converting syngas to light olefins due to its shape selectivity and the match of its pore sizes with those of light olefin molecules [10, 25, 26]. The acidity is an important factor affecting the catalytic performance of SAPO-34 molecular sieves. Molecular sieves with strong acidity are conducive to hydrogen transfer, which may affect the selectivity of reaction products. Besides acidity tuning, the diffusion efficiency is another critical factor that affects the catalytic performance of SAPO-34 in catalytic reaction. Hierarchical SAPO-34 can shorten the residence time of olefin products in the crystals and inhibit the secondary reaction of hydrogen transfer of olefin products, which helps to improve the selectivity of light olefins [27–31]. Post treatment is a common approach to prepare hierarchical SAPO-34 [32–34]. However, the synthesis of hierarchical SAPO-34 in previous studies usually includes the following steps [32–35]: (1) parent SAPO-34 was synthesized by crystallization, washing, drying and calcination; (2) appropriate post-treatment agent was selected to treat parent SAPO-34 through different methods; (3) the as-treated SAPO-34 was then separated by filtration and followed by washing and drying. The overall process of post-treatment is cumbersome and limits its wide application.

In this work, we present a method to obtain hierarchical SAPO-34 by a facile post-treatment in mother liquor at low temperature. The obtained hierarchical SAPO-34 were mixed with ZnCrAlOx oxide to prepare the bifunctional catalyst, the catalytic performance of which for the direct conversion of syngas to light olefins was studied. Compared with the bifunctional catalyst obtained from parent SAPO-34 molecular sieves without post-treatment, the bifunctional catalyst with hierarchical SAPO-34 obtained by mother liquor post-treatment shows better performance. The post-treatment method provides a facial approach for the synthesis of hierarchical SAPO-34 molecular sieves. It also shows a certain reference value for the preparation of other types of hierarchical molecular sieves by the post-treatment method.

2 Experimental Section

2.1 Catalyst Preparation

2.1.1 Fabrication of Hierarchical SAPO-34

Hierarchical SAPO-34 molecular sieves were synthesized with triethylamine as the template under hydrothermal conditions for crystallization in the Teflon-lined stainless steel autoclave. After cooled to room temperature by cold water, the autoclaves were directly transferred to a rotating oven to enable the crystallized products to be post-treated in mother liquor for different time at 40℃.

The molar composition of the starting gels was as follows: SiO_2:Al_2O_3:H_3PO_4:TEA:H_2O = 0.2:1.0:2.0:3.0:50. In a typical synthesis, firstly, 10.12 g pseudoboehmite and 51.7 g water were mixed evenly, then 16.14 g orthophosphoric acid, 2.75 g silica sol and 20.25 g triethylamine were then added slowly under vigorous stirring. The resulting mixture was continuously stirred at room temperature for 2 h. Finally, the resulting mixture was sealed in a 150 mL Teflon-lined stainless steel autoclave. The crystallization was carried out at 200 °C under autogenic pressure for 38 h. After this crystallization process, the autoclaves were taken out from the rotating oven, cooled to room temperature by water, and then put back into the rotary oven at 40 °C for different time. Afterwards, the obtained product was separated by centrifugation, washed with deionized water and dried at 100 °C overnight. Finally, the dried samples were calcined at 550 °C for 6 h to remove the organic template in the muffle furnace. The as-prepared samples were named as SP34-*X* with *X* designating the rotation time (*X* = 20, 40, 80 and 120 min). As a comparison, parent SAPO-34 molecular sieves with traditional microporous structure were prepared as follows: the autoclave was taken from the rotary oven immediately after crystallization and cooled by cold water. The resulting materials were then collected from the autoclave. Other experimental conditions were the same as the treatment process of hierarchical SAPO-34, and the sample was named as SP34-0. The prepared SP34-*X* (*X* = 0, 20, 40, 80 and 120 min) were pressed, crushed and sieved to granules of 40–60 mesh.

2.1.2 Preparation of $ZnCrAlO_x$

$ZnCrAlO_X$ was prepared by co-precipitation method. The specific process is as follows: Zinc source, Chromium source and aluminum source are $Zn(NO_3)_2{\cdot}6H_2O$, $Cr(NO_3)_3{\bullet}9H_2O$ and $Al(NO_3)_3{\cdot}9H_2O$, respectively. 13.47 g $Zn(NO_3)_2{\cdot}6H_2O$, 12.03 g $Cr(NO_3)_3{\cdot}9H_2O$, 11.33 g $Al(NO_3)_3{\cdot}9H_2O$ were dissolved in 150 mL distilled water to form a mixed salt solution. $(NH_4)_2CO_3$ aqueous solution was used as the precipitant. Both solutions were simultaneously added drop by drop to a beaker containing 20 mL deionized water under continuous stirring at 70 °C. By adjusting the addition rate of alkaline solution, the pH value of aqueous solution was maintained at 7.0–8.0. After stirring for 3 h at 70 °C, the precipitate was separated by filtration, washed with deionized water and dried at 60 °C overnight. Finally, the dried samples were calcined at 550 °C for 1 h with a ramping rate of 2 °C /min in the muffle furnace. The obtained ternary oxides were denoted as ZCA. The prepared ZCA was pressed, crushed and sieved to granules of 40–60 mesh.

2.1.3 Preparation of Bifunctional Catalyst

The prepared SAPO-34 molecular sieves (40–60 mesh) were mixed with ZCA metal oxides (40–60 mesh), the mass ratio of metal oxides to molecular sieves is 2:1, and the bifunctional catalyst was named ZCA/SP34-*X* (*X* = 0, 20, 40, 80 and 120 min).

2.2 Catalytic Reaction Tests

Catalytic reaction was performed on a high-pressure fixed-bed stainless steel reactor. Typically, 1 mL of bifunctional catalyst (40–60 mesh) was loaded in a reactor (inner diameter, 8 mm). Prior to the reaction, the catalyst was first reduced for 4 h at 300 °C in H_2 (30 mL· min^{-1}) at 2 MPa. Syngas with a H_2/CO ratio of 2:1 containing 5% Ar was introduced into the reactor. Argon in the syngas was used as the internal standard for the calculation of CO conversion. The reaction temperature is 350, 365, 375 and 400 °C. The reaction pressure is 0.5 MPa, 1.0, 1.5 and 2.0 MPa. Gas hourly space velocity (GHSV) is 3000, 4000, 5000 and 6000 h^{-1}.

Products were analyzed by an online GC (Agilent 7890B), which was equipped with a thermal conductivity detector (TCD) and a flame ionization detector (FID). Hydrocarbons were analyzed using a capillary column (HP-PLOT Al_2O_3) with a flame ionization detector (FID). A packed column (TDX-1) connected to a thermal conductivity detector (TCD) was used to analyze H_2、CO、CH_4、CO_2 and so on. The conversion of CO, selectivity of CO_2 and the selectivity of hydrocarbon (C_pH_q) excluding CO_2 were calculated as follows:

CO conversion was calculated on a carbon atom basis, i.e.

$$Con_{\mathrm{CO}} = \left[\left(CO_{\mathrm{in}} - CO_{\mathrm{out}}\right)/CO_{\mathrm{in}}\right] * 100\%$$

where CO_{in} and CO_{out} represent moles of CO at the inlet and outlet, respectively.

CO_2 selectivity (S_{CO2}) was calculated according to:

$$S_{CO2} = CO_{2out}/(CO_{in} - CO_{out})$$

where CO_{2out} denotes moles of CO_2 at the outlet.

The selectivity of hydrocarbon C_pH_q (S_{CpHq}) was obtained according to:

$$SCpHq = n(CpHq, out)/(\sum\nolimits_{(i=1)}^{p} n(CpHq, out)) * 100\%$$

3 Results and Discussion

3.1 Fabrication of the Hierarchical SAPO-34

Scheme 1 shows schematic illustration of synthetic procedure for the fabrication of hierarchical SAPO-34. Firstly,

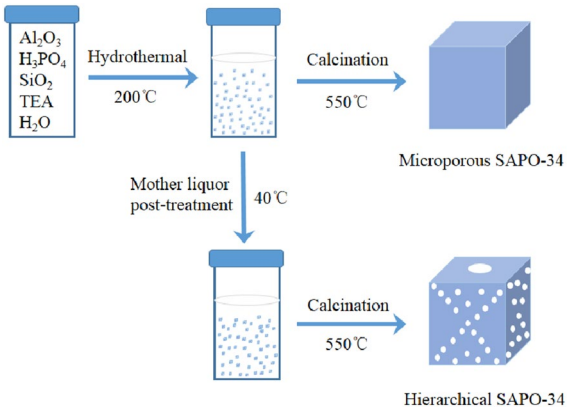

Scheme 1 Schematic illustration of synthetic procedure for the fabrication of hierarchical SAPO-34

the crystallization was completed under hydrothermal conditions at 200 °C. After this crystallization process, a facile and simple post-treatment method was applied to obtain macropores by treating the crystallized product in a facile solution system, mother liquor. Finally, the resulting materials were collected and calcined to remove the organic template in the muffle furnace to obtain the hierarchical SAPO-34.

3.2 XRD analysis of Molecular Sieves

Figure 1 shows the XRD patterns of all samples. In the figure, the diffraction peaks of the synthesized SAPO-34 molecular sieves are consistent with those reported in the literature [36, 37]. The occurrence of weak peaks at 16.9°, 19.6° and 21.3° indicates that the synthesized samples have AEI structure in addition to the standard CHA structure of SAPO-34, which indicates that the synthesized samples are

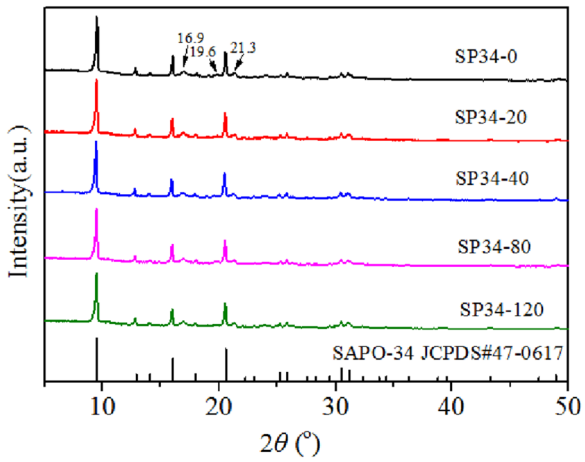

Fig. 1 The XRD profiles of the as-synthesized SP34-*X* molecular sieves (*X* = 0, 20, 40, 80 and 120 min)

intergrowth structure with the CHA/AEI structures. Compared with SP34-0 obtained without mother liquor post-treatment, the characteristic peak of SP34-*X* molecular sieves (*X* = 20, 40, 80 and 120 min) after post-treatment did not change significantly, indicating that the crystal structure of SP34-*X* molecular sieves was largely preserved during the mother liquor post-treatment under our experiment condition.

3.3 SEM and TEM Analysis of the Molecular Sieves

Figure 2 shows the scanning electron microscopy (SEM) images of SP34-*X* (*X* = 0, 20, 40, 80 and 120 min). All of the samples show a typical cubic morphology. The crystal size is uniform, and the particle size is approximately 2–3 um. In contrast to the SP34-0 with smooth crystal surface, it can be clearly observed that the surfaces of SP34-*X* (*X* = 20, 40, 80 and 120 min) become rougher with the extension of post-treatment time. After 20 min of mother liquor post-treatment, butterfly-shape macropore structure can be observed on the crystal surface. With the extension of mother liquor post-treatment time, the etching of crystal

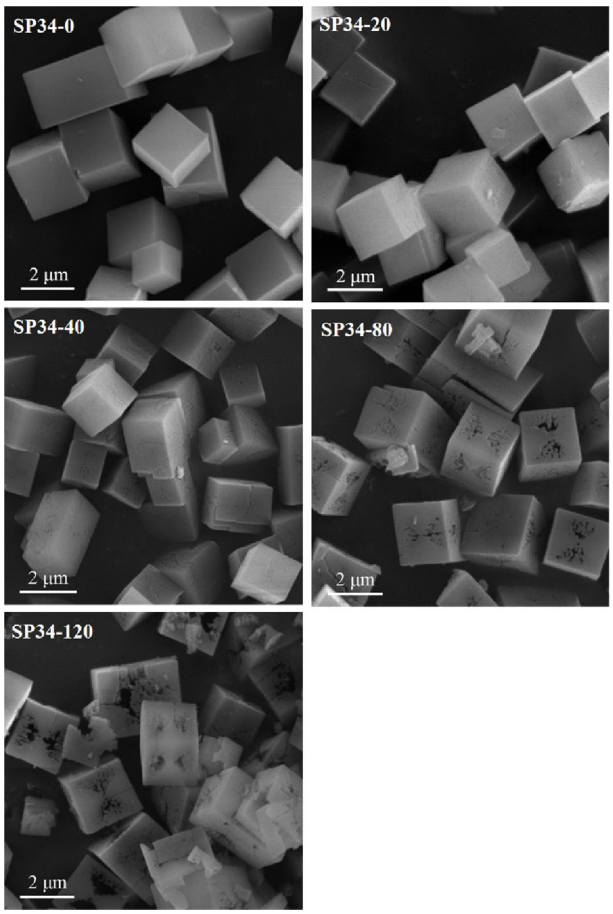

Fig. 2 The SEM images of SP34-*X* (*X* = 0, 20, 40, 80 and 120 min)

surface become more and more notable and butterfly-shape macropore structure become more and more obvious. When the post-treatment time was increased to 120 min, hourglass-shaped macroporous structure could be observed on some crystals. Some crystals even partially dissolved and became fragments due to the long-time mother liquor etching. The TEM images of SP34-*X* (*X* = 0, 20, 40, 80 and 120 min) are shown in Fig. 3. The macropores inside the crystals structure could be clearly observed for samples SP34-*X* (*X* = 20, 40, 80 and 120 min) and become more significant with the extension of mother liquor post-treatment time, which is consistent with the results of SEM.

3.4 Nitrogen Adsorption–Desorption Analysis of Molecular Sieves

Figure 4 and Figure S1 illustrate the N_2 adsorption–desorption isotherms of all samples. Due to the existence of micropores, the adsorption isotherms of all samples have steep uptakes near P/P0 = 0. Different from SP34-0 sample, the adsorption quantity of SAPO-34 molecular sieves obtained by mother liquor post-treatment increases sharply

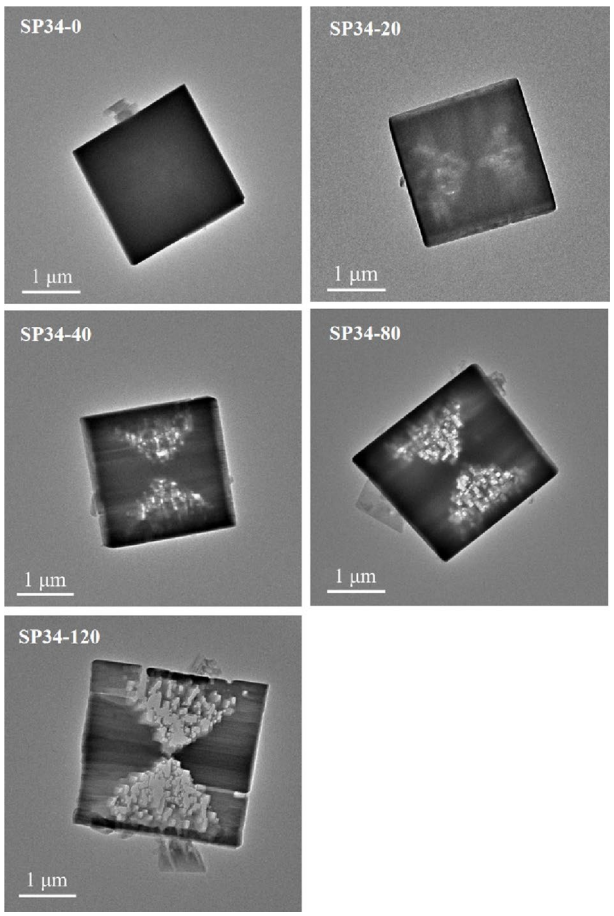

Fig. 3 The TEM images of SP34-*X* (*X* = 0, 20, 40, 80 and 120 min)

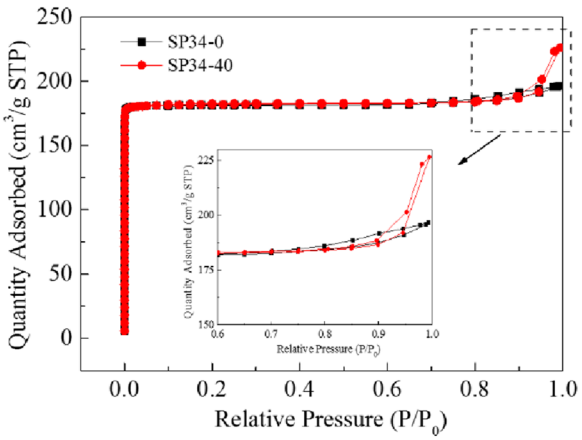

Fig. 4 The N_2 adsorption–desorption isotherms of SP34-0 and SP34-40

under the high pressure of P/P0 > 0.8, indicating the existence of macropores besides mesopores [37, 38]. The specific surface area and pore volume of all samples are shown in Table 1. The mesopore volumes of SP34-*X* (*X* = 0, 20 and 40 min) with the extension of mother liquor post-treatment time gradually increased. With the further increase of mother liquor post-treatment time, mesopore volumes of SP34-*X* (*X* = 80 and 120 min) begin to decrease. However, it should be noted that mesopore volumes of SP34-*X* (*X* = 20, 40, 80 and 120 min) are higher than that of SP34-0, which results from the introduced secondary porosity.

3.5 XRF Analysis of Molecular Sieves

The chemical composition of the calcined SP34-*X* (*X* = 0, 20, 40, 80 and 120 min) molecular sieves is given in Table 1. SP34-*X* (*X* = 20, 40, 80 and 120 min) molecular sieves show the comparable framework compositions with SP34-0. The results demonstrate that the mother liquor treatment is non-selective towards a particular framework cation. Thus, the unbiased chemical dissolution generates a hierarchical material with a composition similar to the parent's material, which is also observed in the results of other studies [39, 40].

3.6 NH_3-TPD Analysis of Molecular Sieves

The acidity of SP34-*X* (*X* = 0, 20, 40, 80 and 120 min) molecular sieves were examined by NH_3-TPD measurements. As shown in Fig. 5, all the samples exhibit two obvious NH_3 desorption peaks. The NH_3 desorption peaks at 188–194 °C and 409–419 °C correspond to the weak acid sites and the strong acid sites, respectively [41, 42]. Compared with the SP34-0, the ammonia desorption profiles of SP34-*X* (*X* = 20, 40, 80 and 120 min) move slightly to the

Table 1 The textural properties and framework composition of the samples

Samples	BET surface area (m^2/g)	Mesopore volume (cm^3/g)	Micropore volume (cm^3/g)	Molar composition
SP34-0	775	0.02	0.28	$Si_{0.056}Al_{0.504}P_{0.440}O_2$
SP34-20	770	0.05	0.28	$Si_{0.054}Al_{0.503}P_{0.443}O_2$
SP34-40	774	0.07	0.28	$Si_{0.054}Al_{0.505}P_{0.441}O_2$
SP34-80	775	0.05	0.28	$Si_{0.056}Al_{0.506}P_{0.438}O_2$
SP34-120	746	0.04	0.27	$Si_{0.059}Al_{0.503}P_{0.438}O_2$

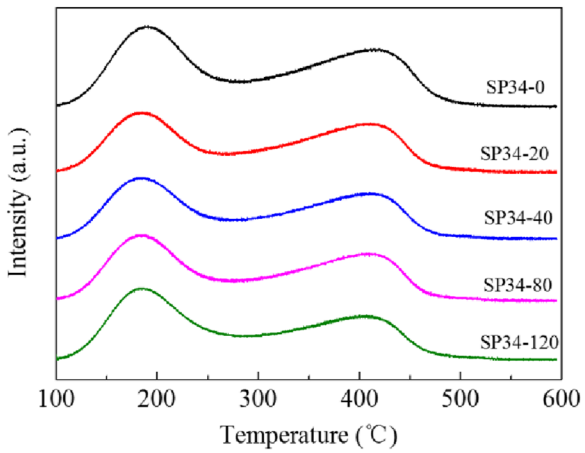

Fig. 5 The NH_3-TPD profiles of SP34-*X* (*X* = 0, 20, 40, 80 and 120 min)

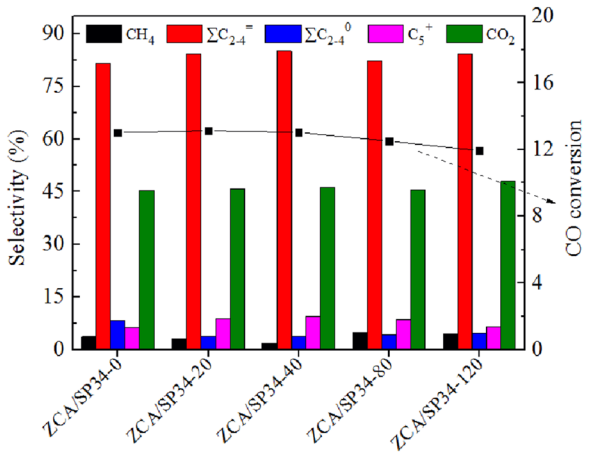

Fig. 6 Catalytic performance (hydrocarbon selectivity is CO_2 free) of ZCA/SP34-*X* (*X* = 0, 20, 40, 80 and 120 min) catalyst. Reaction conditions: T = 350 °C, P = 1.0 MPa, GHSV = 6000 h^{-1}, $H_2/CO = 2$ and weight ratio of metal oxide to SAPO-34 = 2:1.

low temperature direction, indicating that the post-treatment with mother liquor did not sharply change the acidity of SP34-X (X = 20, 40, 80 and 120 min) molecular sieves, which is attributed to the indiscriminate extraction of framework atoms and largely preserved crystallinity.

3.7 Catalytic Performance

Under different reaction conditions, the performance for direct conversion of syngas to light olefins with bifunctional catalyst ZCA/SP34-*X* (*X* = 0, 20, 40, 80 and 120 min) was investigated, as shown in the Fig. 6 and Figure S2. It could be seen from the evaluation results, the bifunctional catalysts prepared by hierarchical SAPO-34 after mother liquor post-treatment showed better performance with higher selectivity of light olefins than the bifunctional catalysts prepared by SP34-0 without mother liquor post-treatment. Among bifunctional catalysts, the catalyst ZCA/SP34-40 showed the best performance with the lowest methane selectivity of about 2%, the highest light olefin selectivity of 85%.The enhanced catalytic performance of ZCA/SP34-40 is ascribed to the introduction of moderate secondary pores. The introduction of hierarchical structure can shorten the length of micropores and increase the rate of mass transfer, thus facilitating the diffusion of intermediates between the ZnCrAlOx catalyst and SAPO-34 or along the SAPO-34 micropores, which can avoid further hydrogenation and conversion of olefin products on the catalyst, thus can improve the selectivity of C_2-C_4 olefins.

Among all the catalysts, ZCA/SP34-40 showed the best catalytic performance. Therefore, we further optimized the process parameters based on ZCA/SP34-40 catalyst, including reaction temperatures, pressures and gas hourly space velocity (GHSV).

The effect of reaction temperature on catalytic performance is shown in Fig. 7. Both the CO conversion and $C_{2-4}^{=}$ selectivity first increased and then decreased slightly with the increase of reaction temperature. When the temperature was increased from 350 °C to 375 °C, the CO conversion increased gradually from 13 to 16%. In addition, when the temperature rose from 350 °C to 365 °C, the selectivity of light olefins was slightly improved. When the temperature continued to rise to 375 °C, the selectivity decreased slightly, while the CO conversion still increased. However, CO conversion and the selectivity of light olefins decreased significantly when the temperature continued to rise to 400 °C, which was possibly due to the limitation of thermodynamic equilibrium [43].

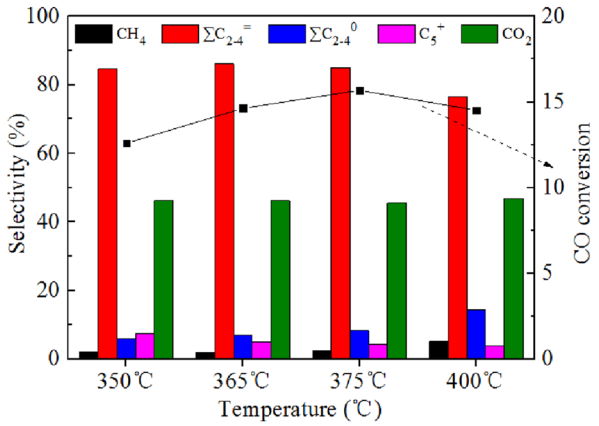

Fig. 7 Effect of reaction temperature of syngas on catalytic behaviors (hydrocarbon selectivity is CO_2 free) of ZCA/SP34-40 catalyst. Other conditions: P = 1 MPa, GHSV = 6000 h^{-1}, $H_2/CO = 2$

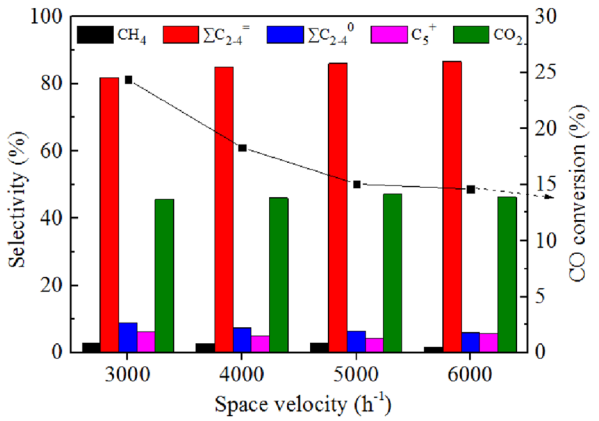

Fig. 8 Effect of space velocity of syngas on catalytic behaviors (hydrocarbon selectivity is CO_2 free) of ZCA/SP34-40 catalyst. Other conditions: P = 1 MPa, T = 365 °C, $H_2/CO = 2$

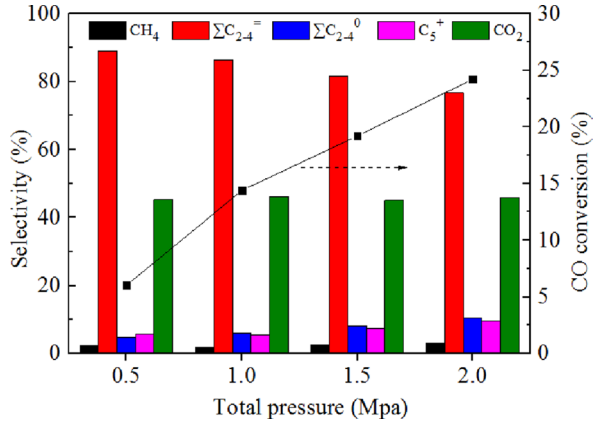

Fig. 9 Effect of total pressure of syngas on catalytic behaviors (hydrocarbon selectivity is CO_2 free) of ZCA/SP34-40 catalyst. Other conditions: T = 365 °C, GHSV = 6000 h^{-1}, $H_2/CO = 2$

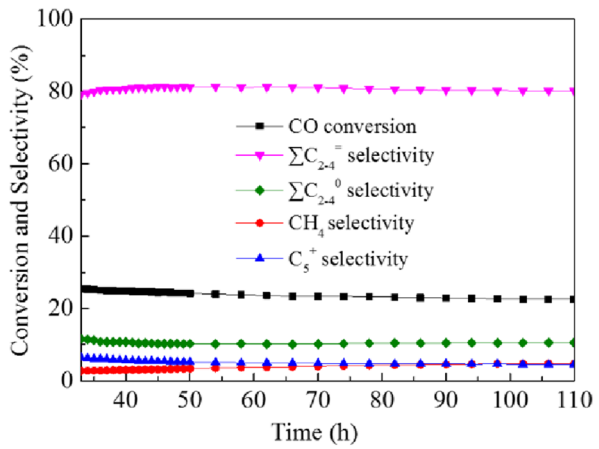

Fig. 10 The stability test (hydrocarbon selectivity is CO_2 free) over the ZCA/SP34-40 catalyst. Reaction conditions: P = 1 MPa, T = 375 °C, GHSV = 3000 h^{-1}, $H_2/CO = 2$

Figure 8 shows the effect of space velocity on catalytic performance. When the space velocity increased from 3000 h^{-1} to 6000 h^{-1}, the CO conversion decreased from 24 to 15%, while the selectivity of light olefins increased from 82 to 87%. The evaluation results showed that the increase of space velocity shortened the contact time between CO and catalyst, resulting in the reduction of CO conversion. At the high space velocity, light olefin products could leave quickly to avoid further hydrogenation and conversion of intermediate products on the catalyst, thus increase the selectivity of light olefins and decrease the selectivity of light alkanes.

The pressure tests were carried out over ZCA/SP34-40 catalyst from 0.5 to 2.0 MPa. The results are shown in Fig. 9. When the reaction pressure increased from 0.5 to 2 MPa, CO conversion increased significantly from 6 to 24%, but the selectivity of light olefins decreased with the increase of reaction pressure. Meanwhile, the selectivity of light alkanes was improved. The experimental results indicate that the increase of the reaction pressure could effectively promote the conversion of CO, which is in accordance with the moving direction of syngas conversion equilibrium. However, the increase of pressure is conducive to the hydrogenation reaction, which can promote the hydrogenation of light olefins, resulting in the decrease of light olefin selectivity and the increase of light alkane selectivity.

3.8 The Stability of ZCA/SP34-40 Bifunctional Catalyst

The ZCA/SP34-40 bifunctional catalyst was also subjected to the catalytic stability evaluation in the syngas conversion into light olefins, as shown in Fig. 10. It was found that the CO conversion and light olefins selectivity

remained stable at the reaction time of 100 h. Above results indicated that the prepared ZCA/SP34-40 bifunctional catalyst exhibited good catalytic stability in the reaction process. Even if the reaction time was extended to 1000 h, the CO conversion did not decrease significantly and remains at 19%, while the selectivity of light olefins decreased to about 63% due to the carbon deposition on SAPO-34 molecular sieves, which further shows that the bifunctional catalyst has good stability, as shown in Figure S4. Additionally, Figure S5 presented the comparison of catalytic stability for ZCA/SP34-0 and ZCA/SP34-40 catalysts. Better catalytic stability was shown in ZCA/SP34-40 catalyst during the course of syngas reaction. Therefore, the bifunctional catalysts prepared by hierarchical SAPO-34 exhibit a prolonged catalytic stability for light olefins, owing to the improved mass transport and decreased coke formation rate.

4 Conclusion

SAPO-34 molecular sieves with a hierarchical structure was successfully synthesized by a facile post-treatment method, i.e., treatment in a facile solution system, mother liquor. The characterizations suggest that the post-treatment method with mother liquor has resulted in crystal etching to generate hierarchical porous structures. In the combination of ZnCrAlOx oxides with the hierarchical SAPO-34 for syngas to light olefins reaction, the bifunctional catalyst (ZCA/SP34-40) prepared by hierarchical SAPO-34 post-treated in mother liquor for 40 min showed the best performance with the lowest methane selectivity of about 2%, the highest light olefin selectivity of 85% in syngas to light olefins reactions, mainly due to the introduction of moderate secondary pores. Besides, the prepared bifunctional catalyst also has good stability. The post-treatment method provides a facile approach for the research of green synthesis of hierarchical SAPO-34 molecular sieves, and also has certain reference significance for the preparation of other types of hierarchical molecular sieves by post-treatment method.

Supplementary Information The online version contains supplementary material available at https://doi.org/10.1007/s10562-022-04245-3.

Acknowledgements This work was supported by the Natural Science Foundation of Liaoning Province (20180550316). The authors gratefully acknowledge Dr. Qixiu Li for revising the English of the manuscript.

Declarations

Conflict of interest The authors declare that they have no known competing financial interests or personal relationships that could have appeared to influence the work reported in this paper.

References

1. Galvis HMT, De Jong KP (2013) Catalysts for production of lower olefins from synthesis gas: a review. ACS Catal 3:2130–2149
2. Zhao Z, Jiang J, Wang F (2021) An economic analysis of twenty light olefin production pathways. J Energy Chem 56:193–202
3. Meng FH, Li XJ, Zhang P et al (2021) A facile approach for fabricating highly active ZrCeZnO in combination with SAPO-34 for the conversion of syngas into light olefins. Appl Surf Sci 542:148713
4. Ye M, Li H, Zhao Y et al (2015) MTO processes development: the key of mesoscale studies. Adv Chem Eng 47:279–335
5. Chen Q, Lv M, Gu Y et al (2018) Hybrid energy system for a coal-based chemical industry. Joule 2:607–620
6. Zhou W, Kang J, Cheng K et al (2018) Direct conversion of syngas into methyl acetate, ethanol, and ethylene by relay catalysis via the intermediate dimethyl ether. Angew Chem Int Ed 57:12012–12016
7. Sun J, Yang G, Peng X et al (2019) Beyond cars: fischer-tropsch synthesis for non-automotive applications. ChemCatChem 11:1412–1424
8. Ni Y, Liu Y, Chen Z et al (2019) Realizing and recognizing syngas-to-olefins reaction via a dual-bed catalyst. ACS Catal 9:1026–1032
9. Zhou W, Cheng K, Kang J et al (2019) New horizon in C1 chemistry: breaking the selectivity limitation in transformation of syngas and hydrogenation of CO_2 into hydrocarbon chemicals and fuels. Chem Soc Rev 48:3193–3228
10. Tian P, Wei YX, Ye M et al (2015) Methanol to olefins (MTO): from fundamentals to commercialization. ACS Catal 5:1922–1938
11. Jiao F, Li JJ, Pan XL et al (2016) Selective conversion of syngas to light olefins. Science 351:1065–1068
12. Cheng K, Gu B, Liu XL et al (2016) Direct and highly selective conversion of synthesis gas into lower olefins: design of a bifunctional catalyst combining methanol synthesis and carbon-carbon coupling. Angew Chem Int Ed 55:4725–4728
13. Zhu YF, Pan XL, Jiao F et al (2017) Role of manganese oxide in syngas conversion to light olefins. ACS Catal 7:2800–2804
14. Li N, Jiao F, Pan XL et al (2019) Size effects of ZnO nanoparticles in bifunctional catalysts for selective syngas conversion. ACS Catal 9:960–966
15. Su JJ, Wang D, Wang YD et al (2018) Direct conversion of syngas into light olefins over zirconium-doped indium (III) oxide and SAPO-34 bifunctional catalysts: design of oxide component and construction of reaction network. ChemCatChem 10:1536–1541
16. Kirilin AV, Dewilde JF, Santos V et al (2017) Conversion of synthesis gas to light olefins: impact of hydrogenation activity of methanol synthesis catalyst on the hybrid process selectivity over Cr-Zn and Cu-Zn with SAPO-34. Ind Eng Chem Res 56:13392–13401
17. Wang S, Wang PF, Shi DZ et al (2020) Direct conversion of syngas into light olefins with low CO_2 emission. ACS Catal 10:2046–2059
18. Liu XL, Wang MH, Yin HR et al (2020) Tandem catalysis for hydrogenation of CO and CO_2 to lower olefins with bifunctional catalysts composed of spinel oxide and SAPO-34. ACS Catal 10:8303–8314
19. Tan L, Wang F, Zhang PP et al (2020) Design of a core-shell catalyst: an effective strategy for suppressing side reactions in syngas for direct selective conversion to light olefins. Chem Sci 11:4097–4105
20. Liu XL, Zhou W, Yang YD et al (2018) Design of efficient bifunctional catalysts for direct conversion of syngas into lower olefins via methanol/dimethyl ether intermediates. Chem Sci 9:4708–4718

21. Jiao F, Pan XL, Gong K et al (2018) Shape-selective zeolites promote ethylene formation from syngas via a ketene intermediate. Angew Chem Int Ed. 57:4692–4696
22. Su JJ, Zhou HB, Liu S et al (2019) Syngas to light olefins conversion with high olefin/paraffin ratio using ZnCrOx/AlPO-18 bifunctional catalysts. Nat Commun 10:1297
23. Wang MH, Wan ZW, Liu SH et al (2021) Synthesis of hierarchical SAPO-34 to improve the catalytic performanceof bifunctional catalysts for syngas-to-olefins reactions. J Catal 394:181–192
24. Tian P, Zhan GW, Tian J et al (2022) Direct CO_2 hydrogenation to light olefins over $ZnZrO_x$ mixed with hierarchically hollow SAPO-34 with rice husk as green silicon source and template. Appl Catal B 315:121572
25. Olsbye U, Svelle S, Bjørgen M et al (2012) Conversion of methanol to hydrocarbons: how zeolite cavity and pore size controls product selectivity. Angew Chem Int Ed 51:5810–5831
26. Xu ST, Zhi YC, Han JF et al (2017) Advances in catalysis for methanol-to-olefins conversion. Adv Catal 61:37–122
27. Izadbakhsh A, Farhadi F, Khorasheh F et al (2009) Key parameters in hydrothermal synthesis and characterization of low silicon content SAPO-34 molecular sieve. Micropor Mesopor Mater 126:1–7
28. Wang PF, Lv A, Hu J et al (2012) The synthesis of SAPO-34 with mixed template and its catalytic performance for methanol to olefins reaction. Micropor Mesopor Mater 152:178–184
29. Zhong JW, Han JF, Wei YX et al (2017) Recent advances of the nano-hierarchical SAPO-34 in the methanol-to-olefin (MTO) reaction and other applications, Catal. Sci Technol 7:4905–4923
30. Sun QM, Xie ZK, Yu JH (2018) The state-of-the-art synthetic strategies for SAPO-34 zeolite catalysts in methanol-to-olefin conversion. Natl Sci Rev 5:542–558
31. Sun QM, Wang N, Guo GQ et al (2015) Synthesis of tri-level hierarchical SAPO-34 zeolite with intracrystalline micro-meso-macroporosity showing superior MTO performance. J Mater Chem A 3:19783–19789
32. Liu GY, Tian P, Xia QH et al (2012) An effective route to improve the catalytic performance of SAPO-34 in the methanol-to-olefin reaction. J Nat Gas Chem 21:431–434
33. Liu X, Ren S, Zeng GF et al (2016) Coke suppression in MTO over hierarchical SAPO-34 zeolites. RSC Adv 34:6
34. Dang SS, Li SG, Yang CG et al (2019) Selective transformation of CO_2 and H_2 into lower olefins over In_2O_3-ZnZrOx/SAPO-34 bifunctional catalysts. Chemsuschem 12:3582–3591
35. Shu R, Liu GJ, Wu X et al (2017) Enhanced MTO performance over acid treated hierarchical SAPO-34, Chinese. J Catal 38:123–130
36. Xu L, Du AP (2008) Wei YX et al u, Synthesis of SAPO-34 with only Si(4Al) species: effect of Si contents on Si incorporation mechanism and Si coordination environment of SAPO-34. Micropor Mesopor Mater 115:332–337
37. Xing AH, Yuan DL, Tian DY et al (2019) Controlling acidity and external surface morphology of SAPO-34 and its improved performance for methanol to olefins reaction. Micropor Mesopor Mater 288:109562
38. Li YX, Huang YH, Guo JH et al (2014) Hierarchical SAPO-34/18 zeolite with low acid site density for converting methanol to olefins. Catal Today 233:2–7
39. Pan YY, Chen GR, Yang GJ et al (2019) Efficient post-synthesis of hierarchical SAPO-34 zeolites via organic amine etching under hydrothermal conditions and their enhanced MTO performance. Inorg Chem Front 6:1299–1303
40. Dang SS, Li SG, Yang CG et al (2019) Selective transformation of CO_2 and H_2 into lower olefins over In_2O_3-ZnZrOx/SAPO-34 bifunctional catalysts. Chemsuschem 12:1–11
41. Wang C, Yang M, Tian P et al (2015) Dual template-directed synthesis of SAPO-34 nanosheet assemblies with improved stability in the methanol to olefins reaction. J Mater Chem A 3:5608–5616
42. Han L, Guo LL, Xue SZ et al (2021) Polyacrylamide-assisted synthesis of hierarchical porous SAPO-34 zeolites with excellent MTO catalytic performance. Micropor Mesopor Mater 311:110676
43. Dagle VML, Dagle RA, Li JJ et al (2014) Direct conversion of syngas-to-hydrocarbons over higher alcohols synthesis catalysts mixed with HZSM-5. Ind Eng Chem Res 53:13928–13934

Authors and Affiliations

Xiaona Wei[1] · Long Yuan[1] · Wenshuang Li[1] · Shitong Chen[1] · Zhiqiang Liu[1] · Shimin Cheng[1] · Li Li[1] · Chuang Wang[1]

✉ Xiaona Wei
weixiaona@ctdmto.com

✉ Wenshuang Li
liwenshuang@ctdmto.com

✉ Chuang Wang
wangchuang@ctdmto.com

[1] Chia Tai Energy Materials (Dalian) Co., Ltd, No. 7 Yingsheng Road, Ganjingzi AreaLiaoning Province, Dalian 116000, People's Republic of China